

Pulse-level noisy quantum circuits with QuTiP

Boxi Li¹, Shahnawaz Ahmed², Sidhant Saraogi³, Neill Lambert⁴, Franco Nori^{4,5}, Alexander Pitchford⁶, and Nathan Shammah⁷

¹Peter Grünberg Institute - Quantum Control (PGI-8), Forschungszentrum Jülich GmbH, D-52425 Jülich, Germany

²Department of Microtechnology and Nanoscience, Chalmers University of Technology, 412 96 Gothenburg, Sweden

³Department of Computer Science, Georgetown University, 3700 O St NW, Washington, DC 20057, United States

⁴Theoretical Quantum Physics Laboratory, RIKEN Cluster for Pioneering Research, Wako-shi, Saitama 351-0198, Japan

⁵Department of Physics, University of Michigan, Ann Arbor, Michigan 48109-1040, USA

⁶Department of Mathematics, Aberystwyth University, Penglais Campus, Aberystwyth, SY23 3BZ, Wales, United Kingdom

⁷Unitary Fund

May 20th, 2021

The study of the impact of noise on quantum circuits is especially relevant to guide the progress of Noisy Intermediate-Scale Quantum (NISQ) computing. In this paper, we address the pulse-level simulation of noisy quantum circuits with the Quantum Toolbox in Python (QuTiP). We introduce new tools in `qutip-qip`, QuTiP's quantum information processing package. These tools simulate quantum circuits at the pulse level, fully leveraging QuTiP's quantum dynamics solvers and control optimization features. We show how quantum circuits can be compiled on simulated processors, with control pulses acting on a target Hamiltonian that describes the unitary evolution of the physical qubits. Various types of noise can be introduced based on the physical model, e.g., by simulating the Lindblad density-matrix dynamics or Monte Carlo quantum trajectories. In particular, we allow for the definition of environment-induced decoherence at the processor level and include noise simulation at the level of control pulses. As an example, we consider the compilation of the Deutsch-Jozsa algorithm on a superconducting-qubit-based and a spin-chain-based processor, also using control optimization algorithms. We also reproduce experimental results on cross-talk

noise in an ion-based processor, and show how a Ramsey experiment can be modeled with Lindblad dynamics. Finally, we show how to integrate these features with other software frameworks.

1 Introduction

Quantum computation and quantum algorithms are deemed to be able to complete tasks that would be harder to achieve with classical resources. However, noise on quantum hardware significantly influences its performance, limiting large-scale applications. Currently, we are in the so-called noisy intermediate-scale quantum (NISQ) computing era [1]. Before we reach the regime of quantum error correction (QEC) [2], quantum algorithms will suffer from quantum and classical noise, e.g., decoherence and noise in classical control signals. Both types of noise lead to errors in the computation and therefore determine the performance of a quantum algorithm. Hence, a realistic simulation of a quantum algorithm needs to incorporate these different types of noise, which can depend strongly on the type of qubit technology [3].

A modern quantum algorithm typically includes both classical and quantum parts [4]. The former can include classical variational subroutines, while the latter is usually represented by a quantum circuit, consisting of a number of gates applied on a quantum state. Many software projects provide the simulation of such circuits including PyQuil [5, 6], Qiskit [7], Cirq [8], ProjectQ [9], and PennyLane [10], among oth-

Boxi Li: b.li@fz-juelich.de

Shahnawaz Ahmed: shahnawaz.ahmed95@gmail.com

Nathan Shammah: nathan@unitary.fund

arXiv:2105.09902v1 [quant-ph] 20 May 2021

ers [11, 12]. However, within these approaches, noise is usually modelled as an additional layer on top of ideal quantum gates, e.g., probabilistically inserting random Pauli gates or a list of Kraus operators to describe a noisy quantum channel.

To improve the performance of a quantum circuit on noisy hardware, it is useful to also perform optimization at the level of control pulses based on the quantum dynamics of the underlying hardware. For this purpose, open-source software packages have been developed to map quantum circuits to control pulses on hardware, allowing for fine-tuning and calibration of the control pulses, such as `qiskit.pulse` [13], `qctrl-open-controls` [14] and `Pulser` [15].

In the realm of simulation, one of the earliest, and most widely used Python packages to simulate quantum dynamics is the Quantum Toolbox in Python, QuTiP [16, 17]. QuTiP provides useful tools for handling quantum operators and simplifies the simulation of a quantum system under a noisy environment by providing a number of solvers, such as the Lindblad master equation solver. An ecosystem of software tools for quantum technology is growing around it [13, 15, 18–24]. Hence, it is a natural base to start connecting the simulation of quantum circuits and the time evolution of the quantum system representing the circuit registers. At the cost of more computing resources, simulation at the level of time evolution allows noise based on the physical model to be included in the realistic study of quantum circuits.

Summary of results In this paper, we illustrate how the new tools in `qutip-qip`¹ can be used to bridge the gap between the gate-level circuit simulation and the simulation of quantum dynamics following the master equation for various hardware models. While a quantum circuit representation and a few specific Hamiltonian models have been available in QuTiP for some time, in this paper, we bridge them with QuTiP solvers and build a pulse-level simulation framework, allowing the simulation of noisy circuits.

Provided a Hamiltonian model and a map between the quantum gate and control pulses, we show how these new tools in `qutip-qip` can be

used to compile the circuit into the native gates of a given hardware, how to generate the physical model described by control pulses and how to use QuTiP’s dynamical solvers to obtain the full-state time evolution, as shown in Figure 1.

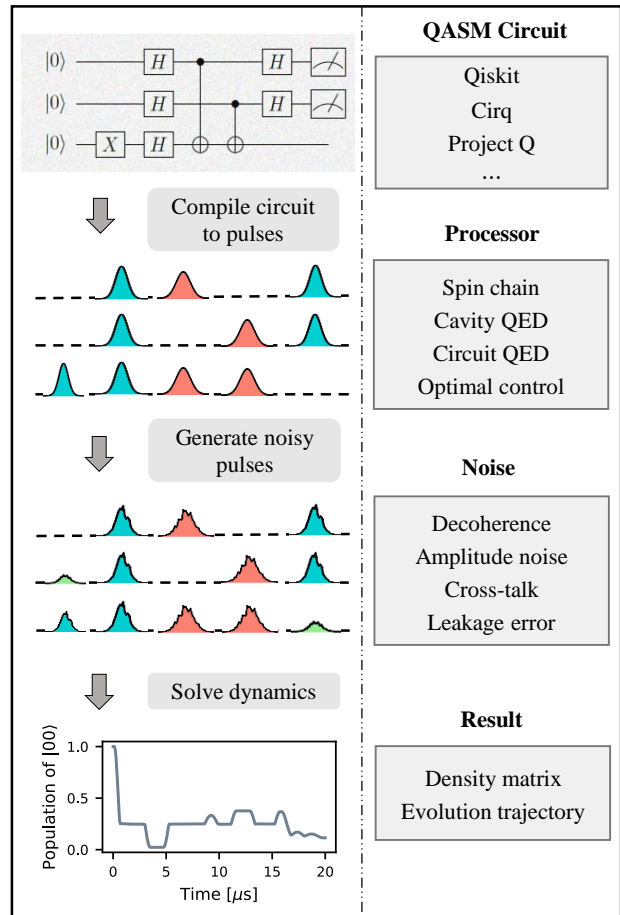


Figure 1: Illustration of the workflow of the pulse-level noisy quantum circuit simulation. It starts from a quantum circuit defined in QuTiP or imported from other libraries through the QASM format. Based on the hardware of interest, the circuit is then compiled to control pulse signals for each control Hamiltonian (blue for single-qubit gates and red for two-qubit gates in the figure). Next, a representation of the time evolution, including various types of noise, is generated under the description of the master equation. In the last step, the QuTiP solver is employed to solve the dynamics. The solver returns the final result as well as the intermediate state information on demand. Both the final and the intermediate quantum states can be recorded, as illustrated by the plot showing the population of the $|00\rangle$ state, with the third qubit traced out. This plot is the same as Figure 8b and will be explained later in detail. The control signals in the figure are for illustration purposes only while the real compiled pulses on a few predefined hardware models are shown in Figure 3.

¹<https://github.com/qutip/qutip-qip>

A number of example hardware models are

available in the software package – a spin qubit processor, a cavity-QED device, a superconducting qubit model – while in general the users are provided with the freedom to define their own devices of choice.

In addition to a predefined map between gates and pulses for each model, optimal control algorithms in QuTiP can also be used to generate control pulses. Moreover, we demonstrate how various types of noise, including decoherence induced by the quantum environment and classical control noise, can be introduced at different layers of the simulation. Thanks to a modular code design, one can quickly extend the toolkit with customized hardware and noise models.

Article structure The article is organized as follows: In Section 2, information about the software installation and specifics is given. In Section 3, we briefly present the theory background of the quantum intermediate representation for quantum circuits, the continuous-time open quantum systems theory and the tools present in `qutip` and `qutip-qip` to represent and simulate them. Section 4 contains the main novel results and new software features: therein, we illustrate in detail the novel architecture of the pulse-level quantum-circuit simulation framework in `qutip-qip` and the available modelling of quantum devices and noise. In Section 5, we show how these features can be integrated with other software through importing external quantum circuits using the QASM format. We conclude in Section 6.

The Appendices contain self-contained code examples: Appendix A shows how to simulate quantum hardware with the `Pulse` description; Appendix B contains the full code for the Deutsch-Jozsa algorithm simulation; Appendix C shows how to customize the physical model of a processor with noise; and Appendix D illustrates how to input and output a quantum circuit in QASM format for full integration with the open-source quantum software ecosystem. More examples can also be found in QuTiP tutorials².

²<http://qutip.org/tutorials.html> under the section Quantum Information Processing

2 Software information

The tools described here are part of the QuTiP project [16, 17]. The `qutip-qip` package builds upon what was once a module of QuTiP, `qutip.qip`. Usage and installation has not significantly changed for the end user, who can easily install the package from the Python package index (PyPI) distribution with

```
pip install qutip-qip
```

Code Listing 1: Installing `qutip-qip`

The `qutip-qip` package has the core `qutip` package as its main dependency. This means that it also builds upon the wider Python scientific open source software stack, including `Numpy` [25] and `Scipy` [26], and optionally `Matplotlib` [27] and `Cython` [28]. `qutip-qip` is a software developed by many contributors [29]. Since Refs. [16, 17], major changes and novelties have been implemented in the QuTiP project development: detailing them goes beyond the scope of this paper and they will be addressed elsewhere.

The `qutip-qip` package is developed with the best practices of open-source software development and scientific software. The codebase is hosted on Github and new code contributions are reviewed by the project maintainers. The license is the new BSD 3.0. The code is thoroughly unit tested, with tests for most objects also run on the cloud in continuous integration, on multiple operating systems. The documentation, whose code snippets and API documentation are also unit tested, can be generated autonomously with Sphinx by forking the QuTiP/`qutip-qip` Github repository.

3 Quantum circuits and open quantum dynamics

In this section, we briefly review the theory of quantum circuits and their modeling on actual devices that are subject to noise. We introduce the formalism of intermediate representation for quantum circuits, then describe the Hamiltonian description at the pulse level, and finally the open-quantum dynamics of a realistic system.

3.1 Quantum circuits and gate-level simulation

A quantum circuit is a model for quantum computation, where the quantum dynamics is abstracted and broken down into unitary matrices (quantum gates), which can be applied to all or only a few circuit registers. Inherited from classical computing, the circuit registers are most often two-level systems, referred to as qubits. The execution of a circuit on a quantum state is then given by

$$|\psi_f\rangle = U_K U_{K-1} \cdots U_2 U_1 |\psi_i\rangle, \quad (1)$$

where $|\psi_i\rangle$ and $|\psi_f\rangle$ are the initial and final state and U_i with $i \in \{1, 2, \dots, K\}$ the quantum gates.

Often, the simulation of quantum circuits is implemented by representing the unitaries and quantum state as complex matrices and vectors. The execution of a circuit is then described as matrix-vector multiplication. We refer to this as gate-level quantum circuit simulation. This gate-level quantum circuit simulation can be performed in `qutip-qip` with the `QubitCircuit` class, which is the Python object used for the quantum intermediate representation of a quantum algorithm.

In order to introduce the effects of noise, quantum states need to be represented by a density matrix and the idea of a quantum channel is introduced, where noise can be characterized by a set of non-unitary Kraus operators acting on the quantum states. Many well-known channel representations of noise have been implemented in circuit simulation, such as depolarising, dephasing, amplitude damping and erasure channel. Although the channel description is very general, noisy gate simulation based on it has two shortcomings.

First, in most implementations, noise is applied after the ideal gate unitaries, while in reality they are not separated. Second, although quantum channels describe the most general evolution that a quantum system can undergo, finding the representation of realistic noise in this channel form is not a trivial task. Usually, a noise channel implemented in simulators only describes single-qubit decoherence and cannot accurately capture the complicated noisy evolution that the system undergoes. Hence, to study the execution of circuits on noisy hardware in more detail, one needs to turn to the quantum dynamics of the hardware platform.

3.2 Continuous time evolution

Down to the physical level, quantum hardware, on which a circuit is executed is described by quantum theory. The dynamics of the system that realizes a unitary gate in Eq. (1) is characterized by the time-evolution of the quantum system. For isolated or open quantum systems, we consider both unitary time evolution and open quantum dynamics. The latter can be simulated either by solving the master equation or sampling Monte Carlo trajectories. Here, we briefly describe those methods as well as the corresponding solvers available in QuTiP.

3.2.1 Unitary time evolution

For a closed quantum system, the dynamics is determined by the Hamiltonian and the initial state. From the perspective of controlling a quantum system, the Hamiltonian is divided into the non-controllable drift H_d (which may be time dependent) and controllable terms combined as H_c to give the full system Hamiltonian

$$H(t) = H_d(t) + H_c(t) = H_d(t) + \sum_j c_j(t) H_j, \quad (2)$$

where the H_j describe the effects of available physical controls on the system that can be modulated by the time-dependent control functions $c_j(t)$, by which one drives the system to realize the desired unitary gates. The shapes of control functions are determined by *control pulses*, such as electric and magnetic field amplitudes driven by laser pulses.

The unitary gate U that is applied to the quantum system driven by the Hamiltonian $H(t)$ is a solution to the Schrödinger operator equation

$$i\hbar \frac{\partial U(t)}{\partial t} = H(t)U(t). \quad (3)$$

By choosing $H(t)$ that implements the desired unitaries (the quantum gates) we obtain a Hamiltonian model for the quantum circuit. The choice of solver depends on the parametrization of the control functions $c_j(t)$. The parameters of $c_j(t)$ may be determined through theoretical models or automated through control optimisation, as described later in Section 4.

3.2.2 Open quantum system dynamics

In reality, a quantum system is never perfectly isolated; hence, a unitary evolution is often only

an approximation. To consider possible interaction with the environment (i.e., an open system), one needs to introduce non-unitary dynamics. One way to describe the evolution of an open quantum system is by the Lindblad master equation. It can be solved either by solving a differential equation (`mesolve`) or by Monte Carlo sampling of quantum trajectories (`mcsolve`). Both can be chosen as a simulation back-end for the pulse-level circuit simulator.

These solvers provide an efficient simulation of open system quantum dynamics under the Born-Markov Secular (BMS) approximations [30, 31], which essentially means that it assumes that the system energies are much larger than the coupling to the environment. For most hardware implementations this noise model is powerful and flexible enough to capture the most salient environmental noise effects.

Lindblad master equation solver. The method `mesolve` solves the dynamics of the “system” density matrix $\rho(t)$ evolving under the coherent evolution provided by Eq. (2), and captures the noise with a Lindbladian described by a set of collapse operators and rates. This can be quite generic, including the possibility for time-dependent rates and collapse operators, but a common example for a quantum circuit consisting of N qubits experiencing relaxation and dephasing would be the master equation,

$$\begin{aligned} \frac{\partial \rho(t)}{\partial t} = & -i[H(t), \rho(t)] + \sum_{j=0}^{N-1} \gamma_j \mathcal{D}[\sigma_j^-] \rho(t) \\ & + \sum_{j=0}^{N-1} \frac{\gamma_j^D}{2} \mathcal{D}[\sigma_j^z] \rho(t), \end{aligned} \quad (4)$$

where H is the system Hamiltonian, γ_j is the relaxation rate of qubit j , γ_j^D the pure dephasing rate of qubit j , $\mathcal{D}[\Gamma_n] \cdot = \Gamma_n \cdot \Gamma_n^\dagger - \frac{1}{2} \Gamma_n^\dagger \Gamma_n \cdot - \frac{1}{2} \cdot \Gamma_n^\dagger \Gamma_n$ is the Lindblad dissipator for a generic jump operator Γ_n , and σ_j^- is the Pauli collapse operator.

This approach allows us to model the coexistence of pulse-level control, in the coherent Hamiltonian part, and the influence of noise. However, the density matrix description of the system introduces a quadratic overhead in memory size. If this becomes a limiting factor for a given simulation, progress can be made by employing the Monte-Carlo quantum trajectory solver, `mcsolve`.

Monte-Carlo quantum trajectories. A popular method that is alternative to the full master equation simulation is the Monte Carlo sampling with quantum trajectories. Noise is included in an effective non-Hermitian Hamiltonian, and a stochastic term is added by pseudo-random sampling. An effective Hamiltonian is continuously applied to the system, integrating the part of Eq. (4) with Lindblad dissipators,

$$H_{\text{eff}} = H(t) - \frac{i}{2} \sum_n \Gamma_n^\dagger \Gamma_n, \quad (5)$$

while the second part is determined stochastically by coin flipping, checking if a random number is greater than the norm of the unnormalized wavefunction. If that is the case, the quantum jump is applied, ensuring the renormalization of the wavefunction,

$$|\psi(t + \delta t)\rangle = \frac{\Gamma_n |\psi(t + \delta t)\rangle}{\sqrt{\langle \psi(t) | \Gamma_n^\dagger \Gamma_n | \psi(t) \rangle}}. \quad (6)$$

The advantage with respect to a Lindblad master equation simulation is that that we need only store the state vector instead of the entire density matrix. Additionally, it also allows simulating the dynamics of single executions instead of the averaged dynamics from a density-matrix simulation using the master equation. A trade-off is present in the number of trajectories that need to be run to evaluate a mean path with a small standard deviation. However, the trajectories can be computed in parallel. QuTiP uses Python’s multiprocessing module to benefit from multi-core computing platforms.

Other dynamical solvers. QuTiP also has solvers for other noise models, such as the (secular and non-secular) Bloch-Redfield equation [30] and the (non-Markovian) hierarchical equation of motion (HEOM) [21, 32]. Current developments in QuTiP are working towards a unified interface to all open system solvers, and these will all then be available as options for noise models in pulse-level circuit simulations.

4 Pulse-level quantum-circuit simulation framework

In this section, we describe the architecture of the simulation framework, which aims at simpli-

fying the simulation of a noisy quantum circuit at the level of the explicit time-evolution of physical qubits. We assume that the physical systems that encode quantum information (qubits) are interacting with a noisy environment in an open quantum system [30, 31]. We then take a modular approach to define and run pulse-level simulations in QuTiP as illustrated in Figure 1 with the following new class definitions:

- **Pulse** describes the pulse parameters, such as shape, Hamiltonian terms, and possible pulse-level noise.
- **Processor** characterizes the physical device that executes a quantum algorithm.
- **Compiler** compiles a quantum circuit to generate a pulse-level description with the available set of pulses.
- **Noise** adds noise to the simulation by modifying the pulses and the Hamiltonian model saved in the processor to tackle classical and quantum noise.

The full architecture is illustrated in Figure 2. The modular components allow defining arbitrary hardware models for quantum computing and simulating their operation using QuTiP.

The **Pulse** class is used to describe possible control pulses in a quantum device. An instance of a **Pulse** packages one term of the Hamiltonian, e.g., σ_x and the explicit array of coefficients $c_j(t)$ on one qubit, see Appendix A. Therefore, a pulse represents a time-dependent control Hamiltonian term $c_j(t)H_j$ in Eq. (2).

The **Processor** represents the underlying quantum system that the pulses will be executed on. Hence, the main workflow is carried out in the **Processor**, just as an experiment running on a quantum device. A **Processor** object contains information about the hardware, e.g., the drift and control Hamiltonians (H_d , H_c), the coherence time (T_1 and T_2) and other information such as whether the pulse should be interpreted as discrete or continuous in the simulation. Such additional information contributes to choices during the simulation, e.g., whether to use a cubic spline interpolation for the coefficients. Pulses can be added to a **Processor** object and then executed using QuTiP solvers described in Section 3.2. The Hamiltonian model here does not

have to be ideal and can already include intrinsic noise such as leakage (see Section 4.4).

On top of this, the connection between the quantum circuit model and the time-evolution is realized by a **Compiler** for the gate-to-pulse compilation. With custom **Compiler** and **Processor** objects, a particular quantum circuit can be converted into a set of pulses to implement the corresponding physical evolution. The starting time for each pulse can be configured and optimized using a **Scheduler**. However, note that decomposing quantum gates to native gate sets and their subsequent compilation and scheduling is very much dependent on the underlying hardware. We provide a set of basic compilers and scheduling strategies but leave it to users to construct more advanced compilers and schedulers for their needs.

Finally, noise due to decoherence or control imperfections in the hardware can be specified using the **Noise** class. A **Noise** object includes additional terms in the Hamiltonian (Eq. (2)) to represent coherent noise sources such as Gaussian noise in the control signal or a parasitic ZZ interaction [33] and collapse operators representing Lindblad noise. We provide some predefined noise models such as **RelaxationNoise**, which adds collapse operators to account for T_1, T_2 relaxation rates in the simulations.

In the following subsections, we describe each module in more detail with partial code snippets to explain their usage. The appendices further contain working code examples for different simulations.

4.1 Pulse

The key feature of the simulator we introduce in this paper is that we simulate the circuit at the level of time evolution, instead of a sequence of unitary matrix multiplications at the circuit level, as in Eq. (1). Therefore the basic elements in our simulation are the control pulses that drive the physical system. Here, we describe how we model a control pulse of the quantum hardware using the class **Pulse** and briefly discuss how to incorporate noise in the pulse.

The control pulses are realized by manipulating the coefficients $c_j(t)$ in Eq. (2). We use the time-dependent Hamiltonian $c_j(t)H_j$ to describe an available control pulse of the quantum hardware to be modelled.

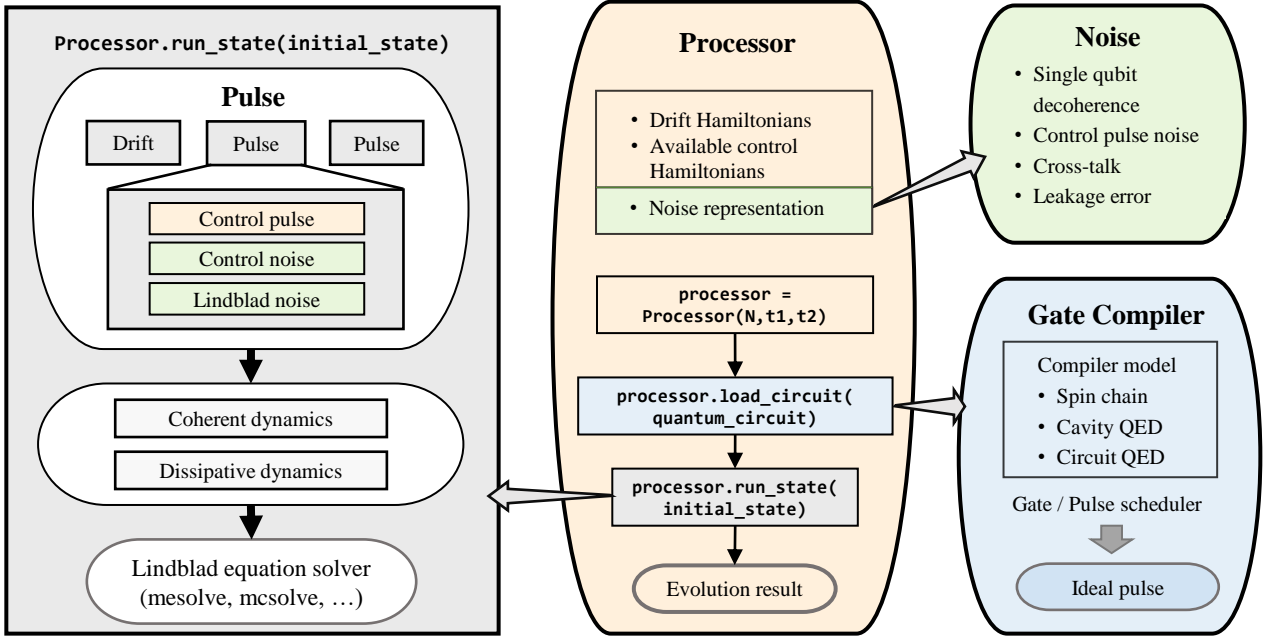


Figure 2: The architecture of the simulation framework. The core of the simulator is `Processor`, which characterizes the quantum hardware of interest, containing information such as the non-controllable drift Hamiltonian and the control Hamiltonians. Apart from the Hamiltonian model representing the qubits, the hardware-dependent `Noise` is also saved in the `Processor`. It describes how noisy terms, such as imperfect control and decoherence, will be added once the control pulse is generated. Some common noise types such as T_1 and T_2 decay can be directly given as parameters for `Processor`. When loading a quantum circuit, the `Compiler` compiles the circuit into a sequence of control pulse signals and schedule the pulse for parallel execution. For each control Hamiltonian, a `Pulse` description is created that includes both the ideal control pulses and the associated noise. They will then be sent to the QuTiP solvers for the computation of time evolution.

Without loss of generality, we can assume that the control Hamiltonian H_j is a constant Hermitian matrix and the time dependency is only on the control function $c_j(t)$. If the Hamiltonian contains oscillations in the off-diagonal terms, it is always possible to divide it into a sum of operators with complex coefficients. As an example, we can write

$$c(t) \begin{pmatrix} 0 & f(t) \\ f^*(t) & 0 \end{pmatrix} = \tilde{c}(t)\sigma^- + \tilde{c}^*(t)\sigma^+ \quad (7)$$

where $f(t)$ is an arbitrary complex function and $\tilde{c}(t) = c(t)f(t)$. This choice of modelling allows more efficient simulation, because only the coefficient is time-dependent.

A simple `Pulse` can be defined in the following way:

```
coeff = np.array([1.])
tlist = np.array([0., np.pi])
pulse = Pulse(
    sigmax(), targets=[0], tlist=tlist,
    coeff=coeff, label="pi-pulse")
```

This code defines a π -pulse implemented using the term σ_x in the Hamiltonian that flips the zeroth qubit specified by the argument `targets`. The pulse needs to be applied for the duration π specified by the variable `tlist`. The amplitude of the pulse is given by the array of coefficients (`coeff`) that is set to the unit.

In addition to the ideal control pulse, we can also define several types of noise in a `Pulse` object, such as Lindblad or control noise, as shown in Figure 2. By control noise we mean additional Hamiltonian terms that result in a coherent noise, i.e., the time evolution is still unitary but is not the desired one. The Lindblad noise, on the other hand, describes the decoherence induced by the environment via superoperators that act on the modelled Hilbert space (Section 3.2.2), for whose representation, however, a larger memory is needed. Lindblad noise can be added to pulses using the method `add_lindblad_noise` and we discuss this further in Section 4.4.

An example of adding a noisy Hamiltonian H_n as control noise through the method

`add_control_noise` is given below:

```
pulse.add_control_noise(
    sigmaz(), targets=[0], tlist=tlist,
    coeff=coeff * 0.05)
```

The above code snippet adds a Hamiltonian term σ_z , which can, for instance, be interpreted as a frequency drift. Similarly, collapse operators are added by a method `add_lindblad_noise`.

In addition to a constant pulse, the control pulse and noise can also be provided as continuous functions and we present examples in appendix A in detail.

Based on this pulse description, we can use various kinds of QuTiP solvers (Section 3.2) to simulate the dynamics of the quantum hardware. However, to simulate quantum circuits, we need two more ingredients: the Hamiltonian model of the quantum hardware (**Processor**) and a compiler that maps the unitary quantum gates to the control pulses (**Compiler**), as discussed in the following two subsections.

4.2 Processor

The **Processor** class characterizes the quantum hardware on which the quantum circuit is executed. As shown in Figure 2, it is the core part of the framework that connects and integrates all related modules. An instance of a **Processor** object contains the information regarding a specific quantum hardware, including the drift Hamiltonian that cannot be controlled, the available control Hamiltonians and possible noise in the system. Therefore we can make a subclass for each physical model.

For the simulation of different quantum hardware, one needs to define the corresponding Hamiltonian model and pass them to an instance of a **Processor**. A few examples have already been implemented: the spin chain model, the qubits-resonator model, the superconducting qubit model (using an effective Hamiltonian [34]) and the optimal control model. While the first three examples are based on specific quantum systems, the optimal control model can take arbitrary control Hamiltonians and use quantum control function optimisation, based on open-loop quantum control theory [35] to find the best pulses.

The following code blocks use the spin chain model to simulate a predefined `circuit` (see Sec-

tion 3.1), written as an instance of **QubitCircuit** using the `qutip-qip` package:

```
processor = LinearSpinchain(
    num_qubits=1, g=1, t2=100)
processor.load_circuit(circuit)
processor.run_state(initial_state)
```

The three lines each correspond to defining a **Processor** model, loading a circuit with the compiler and running the simulation with an initial quantum state (see also Figure 2). Notice that we can also provide the model with parameters like the coupling strength g between the spins and the coherence time t_2 for each qubit. The compilers will be discussed in detail in Section 4.3 and examples of simulating a quantum circuit on a few of these models are shown in Figure 3.

In the following, we explain the predefined hardware models in detail.

4.2.1 Spin Chain model

The spin exchange interaction exists in many quantum systems and is one of the earliest types of interaction used in quantum information processing, e.g., in Refs. [3, 36, 37]. This model implements a system of a few spin qubits with the exchange interaction arranged in a one-dimensional chain layout with either open ends or closed ends.

The interaction is only possible between adjacent qubits. For the spin model, the single-qubit control Hamiltonians are σ_j^x , σ_j^z , while the interaction is realized by the exchange Hamiltonian $\sigma_j^x \sigma_{j+1}^x + \sigma_j^y \sigma_{j+1}^y$. The control Hamiltonian is given by

$$H = \sum_{j=0}^{N-1} \Omega_j^x(t) \sigma_j^x + \Omega_j^z(t) \sigma_j^z + \sum_{j=0}^{N-2} g_j(t) (\sigma_j^x \sigma_{j+1}^x + \sigma_j^y \sigma_{j+1}^y), \quad (8)$$

where Ω^x , Ω^y and g are the time-dependent control coefficients and N is the number of qubits. If the quantum gates act on two qubits that are not adjacent to each other, swap gates will be added to match the topology.

4.2.2 Qubit-resonator model

In some experimental implementations, interactions are realized by a quantum bus or a resonator connecting different qubits. The qubit-resonator

model describes a system composed of a single resonator and a few qubits connected to it. The coupling is kept small so that the resonator is rarely excited but acts only as a mediator for entanglement generation. The single-qubit control Hamiltonians used are σ_x and σ_y . The dynamics between the resonator and the qubits is captured by the Tavis-Cummings Hamiltonian, $\sum_j a^\dagger \sigma_j^- + a \sigma_j^+$, where a , a^\dagger are the destruction and creation operators of the resonator, while σ_j^- , σ_j^+ are those of each qubit. The controllability of the qubit-resonator coupling depends on the physical implementation, but in the most general case we have single and multi-qubit control in the form,

$$H = \sum_{j=0}^{N-1} \Omega_j^x(t) \sigma_j^x + \Omega_j^y(t) \sigma_j^y + g_j(t) (a^\dagger \sigma_j^- + a \sigma_j^+). \quad (9)$$

In the numerical simulation, the resonator Hamiltonian is truncated to finite levels.

4.2.3 Superconducting qubit model

The superconducting qubit is one of the most promising physical qubit implementations [38–40]. In our model, the qubit is simulated by a three-level system, where the qubit subspace is defined as the ground state and the first excited state. The three-level representation will capture the leakage of the population out of the qubit subspace during single-qubit gates. The single-qubit control is generated by two orthogonal quadratures ($a_j^\dagger + a_j$) and $i(a_j^\dagger - a_j)$, truncated to three-level operators. Same as the spin chain model, the interaction is possible only between adjacent qubits. Although this interaction is mediated by a resonator, for simplicity, we replace the complicated dynamics among two superconducting qubits and the resonator with a two-qubit effective Hamiltonian derived in [34].

As an example, we choose the cross resonance interaction in the form of $\sigma_j^z \sigma_{j+1}^x$, acting only on the two-qubit levels. We can write the Hamiltonian as

$$H = H_d + \sum_{j=0}^{N-1} \Omega_j^x (a_j^\dagger + a_j) + \Omega_j^y i (a_j^\dagger - a_j) + \sum_{j=0}^{N-2} \Omega_j^{\text{cr1}} \sigma_j^z \sigma_{j+1}^x + \Omega_j^{\text{cr2}} \sigma_j^x \sigma_{j+1}^z, \quad (10)$$

where the drift Hamiltonian H_d is defined by the anharmonicity α of the second excited state,

$$H_d = \sum_{j=0}^{N-1} \frac{\alpha_j}{2} a_j^\dagger a_j^\dagger a_j a_j. \quad (11)$$

The coefficients Ω^{cr1} and Ω^{cr2} are computed from the qubit-resonator detuning and coupling strength [34]. With additional single-qubit gates, a CNOT gate can be realized using this type of interaction [41]. Using this effective Hamiltonian significantly reduces the size of the Hilbert space in the simulation and allows us to include more qubits. This flexibility in choosing different levels of detail in the modelling is one of the biggest advantages of this framework, in particular for noise simulation (see Section 4.4).

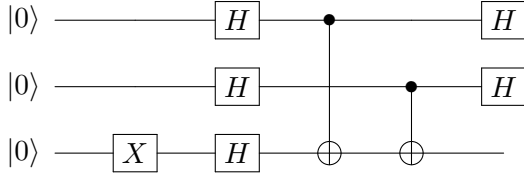
4.2.4 Optimal control model

In addition to using a predefined Hamiltonian model and a gate-to-pulse map, `Processor` can also use the optimal control module in QuTiP. For a set of given control Hamiltonians H_j , the optimal control module uses classical algorithms to optimize the control function $c_j(t)$ in Eq. (2). Parameters of control pulses for realizing individual gates, sequences and hence complete algorithms, are generated automatically through multi-variable optimization targeting maximum fidelity with the evolution described by the circuit.

The optimal control model supports both the GRAPE [23, 42] and the CRAB algorithms [43, 44] that are implemented in the QuTiP library. In this model, one needs to first provide the available control Hamiltonians that characterize the physical controls on the system. Upon loading the quantum circuit, each quantum gate will be passed to the optimal control algorithm as a desired target and the returned pulses that drive this are concatenated to complete a full circuit simulation of physical control sequences.

4.3 Compiler

The compiler converts the quantum circuit to the corresponding control pulses based on the quantum hardware. In this simulation framework, the compilation procedure is achieved through the following steps. First, each quantum gate is decomposed to the native gate set (e.g., rotation

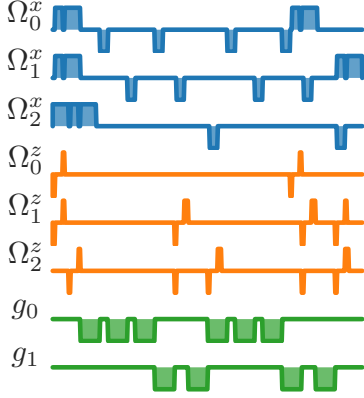


(a) Quantum circuit example

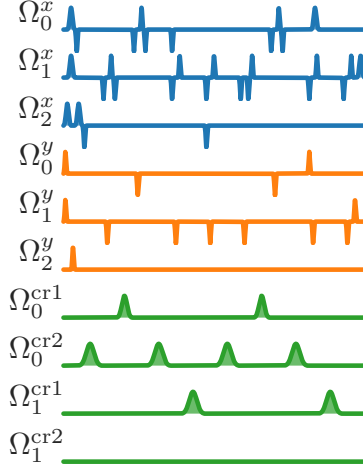
Ω_j^α Single-qubit rotation around an axis $\alpha = x, y, z$ (color blue and orange)

g_j Coupling strength (color green)

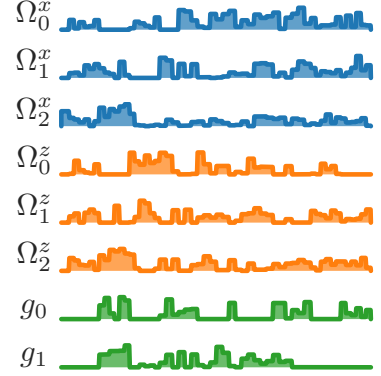
$\Omega_j^{\text{cr}k}$ The cross-resonance effective interaction (color green)



(b) Spin chain model



(c) Superconducting qubit model



(d) Optimal control model

Figure 3: Control pulses generated for a three-qubit Deutsch-Jozsa algorithm (Figure 3a), where two CNOT gates implement the oracle, which is a balanced function. The pulses are compiled using the spin chain model [Section 4.2.1], the superconducting qubits [Eq. (10)] and the optimal control algorithm (using GRAPE with the same control Hamiltonian as the spin chain model in Section 4.2.1). The symbols for pulse coefficients are defined in the corresponding equations. The blue and orange colors denote the two single-qubit control pulses, while green is used for the qubit-qubit interaction. For the spin chain and superconducting qubits, the interaction exists only between neighbouring qubits, hence SWAP gates are added to implement the CNOT between the first and third qubits and decomposed into the native gates. This demonstrates the possibility of simulating noisy quantum circuits on different hardware platforms with various native gate sets under this framework. The strength of the compiled pulses, $|c_j(t)|$, is normalized for plotting and should not be compared between different control Hamiltonians. Code examples generating these plots are shown in appendix B.

over x, y axes and the CNOT gate), with the help of the existing decomposition scheme in QuTiP. If a gate acts on two qubits that are not physically connected, like in the chain model, SWAP gates are added to match the topology before the decomposition. A compiler then maps each quantum gate to the corresponding control-pulse description. In the end, a pulse scheduler is used to explore the possibility of executing multiple quantum gates in parallel.

For the predefined physical models described in the previous subsection, the corresponding compilers are also included. They will be used when calling the method `Processor.load_circuit`, as shown in Figure 2.

As an example, we compile a three-qubit Deutsch-Jozsa algorithm, shown in Figure 3a, while the compiled pulses on three different models are plotted in Figures 3b to 3d. From the plots, it is evident that the same circuit is compiled to completely different control pulses:

- For the spin chain model (Figure 3b), SWAP gates are added between and after the first CNOT gate, swapping the first two qubits (coefficient g_0). The SWAP gate is decomposed into three iSWAP gates, while the CNOT is decomposed into two iSWAP gates plus additional single-qubit corrections. Both the Hadamard gate and the two-qubit gates need to be decomposed to

native gates (iSWAP and rotation on the x and z axes). The compiled signals are square pulses and the control coefficients on σ_z and σ_x are also different, resulting in different gate times.

- For the superconducting qubits (Figure 3c), the compiled pulses have a Gaussian shape. This is crucial for superconducting qubits because the second excited level is only slightly detuned from the qubit transition energy. A smooth pulse usually prevents leakage to the non-computational subspace. Similar to the spin chain, SWAP gates are added to switch the zeroth and first qubit and one SWAP gate is compiled to three CNOT gates. The pulse $\Omega_1^{\text{cr}2}$ (defined in Eq. (10)) is not used because there is no CNOT gate that is controlled by the second qubit and acts on the first one.
- For the optimal control model (Figure 3d), we use the GRAPE algorithm, where control pulses are piece-wise constant functions. We provide the algorithm with same the control Hamiltonian model used for the spin chain model, Eq. (8). In the compiled optimal signals, all controls are active (non-zero pulse amplitude) during most of the execution time. We note that for identical gates on different qubits (e.g., Hadamard), each optimized pulse is different, demonstrating that the optimized solution is not unique, and there are further constraints one could apply, such as adaptations for the specific hardware.

After the circuits are compiled to control pulses, a scheduler is applied to determine the starting time of each pulse. The heuristic scheduling algorithm we provide offers two different modes: ASAP (as soon as possible) and ALAP (as late as possible).

If two gates in the circuit do not commute, the second gate is considered dependent on the first gate. We represent this dependency among quantum gates in the circuit as a directed acyclic graph and allow the permutation of commuting quantum gates. The algorithm then determines the starting time of the control pulse for each quantum gate. In addition, we allow customized constraints on the control system, e.g., two control pulses cannot be turned on at the same time

because they use the same laser. Since the algorithm is heuristic, it does not always return the best solution in one run. Hence, we also offer the option to randomly shuffle the commuting gates for better performance.

To end this subsection, we mention that the gate decomposition is not fully optimized in QuTiP. Circuit optimization at the level of quantum gates, such as for an optimal number of two-qubit gates and more advanced scheduling, depends on the hardware of interest and is still an open research topic [45–48]. Because the focus of this simulator is the simulation of the circuit at the physics level, we leave more advanced optimization and scheduling techniques for future work. Instead, we offer the possibility to import quantum circuits defined in other libraries into QuTiP in QASM format (see Section 5). This allows possible optimizations elsewhere and then exporting the optimized circuits in QuTiP for a pulse-level simulation.

4.4 Noise

The modules described in the previous subsections are sufficient to simulate the execution of quantum circuits on noiseless quantum hardware at the level of time evolution of quantum states. However, one of the greatest benefits of simulating a circuit at the time-evolution level is to introduce a realistic noise model.

The noise module allows one to include and exclude different types of noise, in order to systematically study their effects. Furthermore, as described in Section 4.1, noise can be associated with the control pulses and becomes correlated with the control pulse strength.

Compared to the gate-based simulator (Section 3.1), this framework provides a more practical and straightforward way to describe the noise, based on the physical model. Here, noise can be added at different layers of the simulation, allowing one to focus on the dynamics of the dominant noise, while representing other noise, such as single-qubit relaxation, as collapse operators for efficiency. Depending on the problem studied, one can devote the computing resources to the most relevant type of noise. In the following, we detail the three different noise models in this framework.

Noise in the hardware model. The Hamiltonian model defined in the `Processor` may contain intrinsic imperfections of the system and hence does not implement the ideal unitary gate. Therefore, building a realistic Hamiltonian model usually already introduces noise to the simulation. An example is the superconducting qubits (Section 4.2.3), where the qubit is represented by a three-level system. Since the second excitation is only weakly detuned from the qubit transition, the population may leak out of the qubit subspace. Another example, also implemented for the superconducting qubits, is an always-on ZZ type cross-talk noise due to the interaction with higher levels [33]. Both examples of noise are included in the simulation of the Deutsch-Jozsa algorithm in appendix B

Control noise. The control noise, as the name suggests, arises from imperfect control of the quantum system, such as the pulse amplitude or frequency drift. It is described by the control noise part of `Pulse` (Section 4.1) and results in a discrepancy between the real unitary evolution and the ideal one. The simplest example is noise on the control coefficient $c_j(t)$ in Eq. (2).

As a demonstration of control noise, we simulate classical cross-talk-induced decoherence between two neighbouring ion trap qubits described in [49]. We build a two-qubit `Processor`, where the second qubit is detuned from the first one by $\delta = 1.852$ MHz. A sequence of π -pulses with Rabi frequency of $\Omega = 20$ KHz and random phases are applied to the first qubit. We define noise such that the same pulse also applies to the second qubit. Because of the detuning, this pulse does not flip the second qubit but subjects it to a diffusive behaviour, so that the average fidelity of the second qubit with respect to the initial state decreases. This decreasing fidelity is shown experimentally in Figure 3a of Ref. [49].

Here, we reproduce these results with our two-qubit `Processor` in Figure 4. We start with an initial state of fidelity 0.975 and simulate the Hamiltonian

$$H = \Omega(t)(\sigma_0^x + \lambda\sigma_1^x) + \delta\sigma_1^z, \quad (12)$$

where λ is the ratio between the cross-talk pulse's amplitudes. The plot in Figure 4 shows a similar fidelity decay curve as the experimental result, but includes only the contribution of cross-talk, while in the experimental result other noise

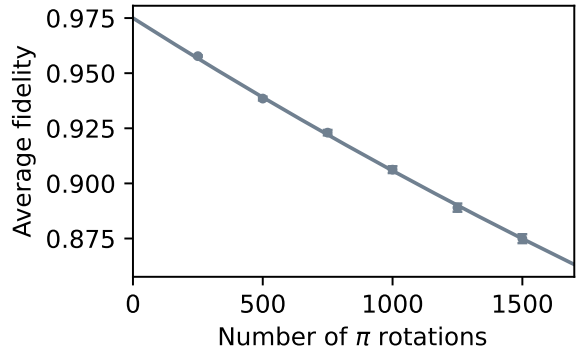


Figure 4: An example of simulated classical cross-talk-induced decoherence between neighbouring qubits in an ion trap system. The randomized benchmarking protocol is adopted from Piltz *et al.* [49] and the figure reproduces the measured fidelity decay in figure 3a of that work. We build a custom `Processor` and `Noise` object to define classical cross-talk noise and perform our simulations. It shows the average fidelity of the qubit when a sequence of single-qubit π rotations with random phase is applied to its direct neighbour. The cross-talk is simulated by adding control pulses to the neighbouring qubits with a strength proportional to that of the target qubit and detuned by the difference of the qubit transition frequency. Each point is sampled from 1600 repetitions. We set the detuning $\delta = 1.852$ MHz, the Rabi frequency $\Omega = 20$ KHz and the cross-talk ratio $\lambda = 1$.

sources may exist. This kind of simulation provides a way to identify noise contribution from different sources. The code is described in detail in appendix C.

Lindblad noise. The Lindblad noise originates from the coupling of the quantum system with the environment (e.g., a thermal bath) and leads to loss of information. It is simulated by collapse operators and results in non-unitary dynamics [30, 31].

The most commonly used type of Lindblad noise is decoherence, characterized by the coherence time T_1 and T_2 (dephasing). For the sake of convenience, one only needs to provide the parameter `t1`, `t2` to the processor and the corresponding operators will be generated automatically. Both can be either a number that specifies one coherence time for all qubits or a list of numbers, each corresponding to one qubit.

For T_1 , the operator is defined as $a/\sqrt{T_1}$ with a as the destruction operator. For T_2 , the operator is defined as $a^\dagger a \sqrt{2/T_2^*}$, where T_2^* is the pure dephasing time given by $1/T_2^* = 1/T_2 - 1/(2T_1)$.

In the case of qubits, i.e., a two-level system, the destruction operator a is truncated to a two-level operator and is consistent with Eq. (4).

In order to demonstrate the simulation of decoherence noise, we build an example that simulates a Ramsey experiment as a quantum circuit run on a noisy `Processor`. The Ramsey experiment consists of a qubit that is initialized in the excited state, undergoes a $\pi/2$ pulse rotation around the x axis, idles for a time t , and is finally measured after another $\pi/2$ pulse rotation. For simplicity, here we only keep the idling part and directly calculate the expectation value with respect to measuring the state $|+\rangle = \frac{1}{\sqrt{2}}(|0\rangle + |1\rangle)$:

```
# define a circuit with only idling
t = 30.
circuit = QubitCircuit(1)
circuit.add_gate("IDLE", 0, arg_value=t)
# define a processor with t2 relaxation
f = 0.5
t2 = 10 / f
processor = LinearSpinChain(1, t2=t2)
processor.add_drift(
    2*np.pi*sigmaz()/2*f, targets=[0])
processor.load_circuit(circuit)
# Record the expectation value
plus_state = \
    (basis(2,1) + basis(2,0)).unit()
result = processor.run_state(
    init_state=plus_state,
    tlist = np.linspace(0., t, 1000),
    # observable
    e_ops=[plus_state*plus_state.dag()])
```

In the above block, we use the linear spin chain processor just for convenience and do not use any of its default Hamiltonians. Instead, we define an always-on drift Hamiltonian σ^z with frequency $f = 0.5$ MHz, and coherence time $T_2 = 10/f$. The obtained expectation value as a function of time is shown in Figure 5 with the solid curve. As expected, the envelope follows an exponential decay characterized by the theoretical prediction characterized by T_2 (dashed curve).

A `Processor` with the decoherence defined in the above way can then be used to simulate quantum circuits. In appendix B, we illustrate the effect of decoherence in the simulation of the 3-qubit Deutsch-Jozsa algorithm. More advanced decoherence noise can be included by using the `add_lindblad_noise` method of `Pulse`.

To end this subsection, we point out that because of the design of the class `Pulse` (Section 4.1), noise can depend on the ideal control

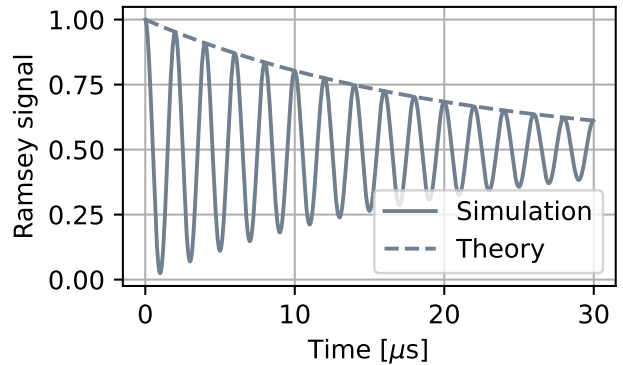


Figure 5: Simulated Ramsey experiment. The quantum system is subjected to a rotation around the z axis of the frequency $f = 0.5$ MHz. The decoherence time is defined as $10/f$. We use a circuit consisting of only an idling gate. The solid line is the population of the state $\frac{1}{\sqrt{2}}(|0\rangle + |1\rangle)$. The dashed line is the theoretical prediction following $(e^{-t/T_2} + 1)/2$.

pulse. Both control noise and Lindblad noise can be defined in a time-dependent way that correlates with a certain control pulse. Using this feature, we have more flexibility in simulating noise, e.g., defining additional decoherence induced by control pulses.

4.5 Adding custom hardware models

As it is impractical to include every physical platform, we provide an interface that allows one to customize the simulators. In particular, the modular architecture allows one to conveniently overwrite existing modules for customization.

To define a customized hardware model, the minimal requirements are a provided Hamiltonian model, i.e., a set of available control Hamiltonians H_j , and a compiler, i.e., the mapping between native gates and control coefficients c_j . One can either modify an existing model or write a model from scratch by subclassing the two parent classes `ModelProcessor` and `GateCompiler`, in which the default simulation workflow is already defined, such as the `load_circuit` method.

Moreover, this customization is not limited to Hamiltonian models and compiler routines. In principle, measurement can be defined as a customized quantum gate and the measurement statistics can be extracted from the obtained density matrix. A new type of noise can also be implemented by defining new `Noise` subclasses, which takes the ideal control pulse and adds noisy

dynamics on top of it.

An example of building customized `Processor` and `Compiler` with new types of noise is provided in appendix C.

5 Importing and exporting circuits in QASM format

As pointed out in Section 4.3, it is impractical to include all the advanced techniques for circuit optimization and scheduling. To allow integration with other packages, we support importation and exportation of circuits in the intermediate Quantum Assembly Language (QASM) format [50]. While there are different intermediate representations for quantum circuits including cQASM [51], QuTiP provides support for OpenQASM. OpenQASM is an imperative programming language that can be used to describe quantum circuits in a back-end agnostic manner.

QuTiP includes a module to import and export quantum circuits compatible with the OpenQASM 2.0 standard [52]. OpenQASM 2.0 allows concise quantum circuit definitions including useful features like custom unitaries and defining groups of qubits over which a common gate can be applied simultaneously. Due to compatibility with multiple libraries such as Qiskit and Cirq, it is an easy way to transfer quantum circuits between these libraries and QuTiP. A simple example of a OpenQASM 2.0 circuit implementing a qubit swap is provided in Figure 6. Furthermore, a code example for importing and exporting OpenQASM 2.0 circuits in QuTiP is provided in appendix D.

6 Conclusion

In this work, we presented a framework for pulse-level quantum circuit simulation that can be used to study noisy quantum devices simulated on classical computers. This framework builds on existing solvers and the quantum circuit model offered by QuTiP. We expanded the noise modeling capabilities with ad-hoc features for the simulation of controls in noisy quantum circuits, such as providing the option to inject coherent noise in pulses.

We provided a few predefined quantum hardware models, compiling and scheduling routines,

```
OPENQASM 2.0;
include "qelib1.inc";

qreg q[2];

cx q[0], q[1];
cx q[1], q[0];
cx q[0], q[1];
```

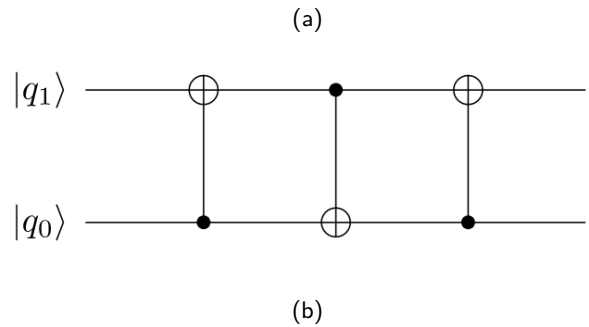


Figure 6: The OpenQASM 2.0 code (a) and corresponding quantum circuit rendered in QuTiP (b) for a simple circuit swapping two qubits.

as well as noise models, which can be adjusted to devote limited computing resources to the most relevant physical dynamics during the study of noise. We benchmarked the simulation capabilities by illustrating how results obtained on cross-talk noise characterization for an ion-trap-based quantum processor can be easily replicated with this toolbox. Moreover, we provided an example of the simulation of Lindblad noise for a Ramsey experiment.

Due to the modular design, the framework here introduced can be integrated with more hardware models, gate decomposition and optimization schemes. In particular, the simulation of processors supporting bosonic models for quantum information processing, including quantum error correction schemes, is especially suitable within the current framework. Represented as customized gates, state preparation and measurement can also be simulated as a noisy physical process.

Pulse-level simulation could be helpful in quick verification of experimental results, developing quantum algorithms, such as variational quantum algorithms [4, 53, 54], and testing compiling and scheduling schemes [55] with realistic noise models. Through hardware simulation and noise simulation, quantum error correction code and quantum mitigation protocols can also be studied, for example, simulating pulse-level and digital zero-

noise extrapolation [56–58].

Moreover, the noise characterization in model devices and the impact of non-Markovian types of noise could be further evaluated [21, 59]. This approach also has a potential to be integrated with other quantum control software such as `qupulse` [60] and `C3` [61]. In particular, the features here introduced may be a useful tool to investigate from a novel perspective many-body dynamical properties of quantum circuits, such as for measurement-induced phase transitions [62], chaotic dynamics and information scrambling [63].

Planned developments in `qutip` and `qutip-qip` will enable the use of alternative quantum control optimization algorithms, that is options other than the GRAPE and CRAB algorithms that are currently supported. Most immediately Krotov-type algorithm support will be added through integration with `qucontrol-krotov` [19], which is already closely aligned with QuTiP. Further plans for QuTiP include the development of an implementation of the GOAT algorithm [64], in which `qutip`'s solvers of all kinds can be used effectively. This will then also be available for optimization of circuit controls to simulate universal gate operations [65, 66].

Another direction of development is the integration with other software frameworks, in the ecosystem of quantum open source software, where considerable duplication exists. Even with respect to the quantum intermediate representation of quantum circuits, standards are not yet solidified. For example, we have connected `qutip-qip` with OpenQASM 2.0, thus providing an access point to any major framework. More sophisticated features are expected in the upcoming OpenQASM 3.0 standard [67], including classical computation specifications and the option for pulse-level definitions for gates. Extending QuTiP support to OpenQASM 3.0 will be an important step in cross-package compatibility with respect to pulse-level quantum circuit simulation and their integration with real hardware.

The use of `qutip-qip` for open quantum hardware is an especially intriguing direction of research and development. One could envision this framework as the backbone for API interconnectivity between simulation and hardware control in research labs with different technolo-

gies [60].

Acknowledgements

We would like to thank the whole community of contributors and users of the QuTiP project and in particular those who developed the quantum circuit representation in the `qutip.qip` module [29] – in particular Anubhav Vardhan, Robert Johansson, and Paul Nation. We also thank Jake Lishman, Èric Giguère, and Simon Cross for work on the QuTiP project. We thank Andrea Mari, Anton Frisk Kockum, Daniel Burgarth, Sebastian Grijalva for useful discussions and comments on the manuscript. Part of this code development has been supported by NumFOCUS and Google Summer of Code. F. N. is supported in part by Nippon Telegraph and Telephone Corporation (NTT) Research, the Japan Science and Technology Agency (JST) [via the Quantum Leap Flagship Program (Q-LEAP), the Moonshot R&D Grant Number JPMJMS2061, and the Centers of Research Excellence in Science and Technology (CREST) Grant No. JPMJCR1676], the Japan Society for the Promotion of Science (JSPS) [via the Grants-in-Aid for Scientific Research (KAKENHI) Grant No. JP20H00134 and the JSPS–RFBR Grant No. JPJSBP120194828], the Army Research Office (ARO) (Grant No. W911NF-18-1-0358), the Asian Office of Aerospace Research and Development (AOARD) (via Grant No. FA2386-20-1-4069), and the Foundational Questions Institute Fund (FQXi) via Grant No. FQXi-IAF19-06. N. S. acknowledges partial support from the U.S. Department of Energy, Office of Science, Office of Advanced Scientific Computing Research, Accelerated Research in Quantum Computing under Award Number de-sc0020266. S. A. acknowledges support from the Knut and Alice Wallenberg Foundation through the Wallenberg Centre for Quantum Technology (WACQT).

Data availability

The code examples present in the Appendices are available at github.com/boxili/qutip-qip-paper. A version compatible with the latest distribution of `qutip-qip` can be found at github.com/qutip/qutip-qip.

A Simulating quantum hardware with Pulse description

In Section 4.1, we introduced our modelling of a quantum hardware using `Pulse`. Here we show a few code examples of using the framework to build a simulation for a single qubit.

We use the toolkit as part of the Python package `qutip-qip`, which can be installed with the following command:

```
pip install qutip-qip
```

The following code block builds a `Processor` for a single qubit with `Pulse` description:

```
import numpy as np
from qutip_qip.device import Processor
from qutip import sigmaz, sigmax, basis
from qutip_qip.pulse import Pulse

processor = Processor(1)
coeff = np.array([1.])
tlist = np.array([0., np.pi/2])
pulse = Pulse(
    sigmax(), targets=0, tlist=tlist,
    coeff=coeff, label="sigmax")
processor.add_pulse(pulse)
plot_time = np.linspace(0, np.pi/2, 20)
solver_result = processor.run_state(
    init_state=basis(2, 0),
    tlist=plot_time)
```

As described in Section 4.1, a `Pulse` consists of the Hamiltonian, the indices of the target qubits, the time sequence and the pulse strength. The `tlist` defines the time sequence and `coeff` the strength of the pulse for each time slot. In the above example, we define a half- π pulse with a Hamiltonian σ_x that is turned on from $t = 0$ to $t = \pi/2$ with strength 1. We also give the pulse a label "sigmax" that can be used to identify the pulse. The evolution of the qubit system under the given control pulse is obtained using the method `run_state`, where we specify the initial state as $|0\rangle$.

Apart from a discrete pulse, it is also possible to define a continuous pulse by specifying the `spline_kind` attribute of `Processor`:

```
# continuous pulse
processor = Processor(1)
processor.pulse_mode = "continuous"
processor.add_control(sigmax())
tlist = np.linspace(0., np.pi/2, 21)
coeff = np.array(np.sin(2*tlist) * np.pi/2)
processor.pulses[0].tlist = tlist
processor.pulses[0].coeff = coeff
solver_result2 = processor.run_state(
    init_state=basis(2, 0),
    tlist=plot_time)
```

The discrete and continuous pulses are plotted in Figure 7.

B Simulating the Deutsch-Jozsa algorithm

In this section, we show the code example of simulating the 3-qubit Deutsch-Jozsa algorithm on three different hardware models: the spin chain model, the superconducting qubits, and the optimal control model:

```
import numpy as np
import matplotlib.pyplot as plt
np.random.seed(0)
from qutip_qip.device import OptPulseProcessor, LinearSpinChain, SCQubits
```

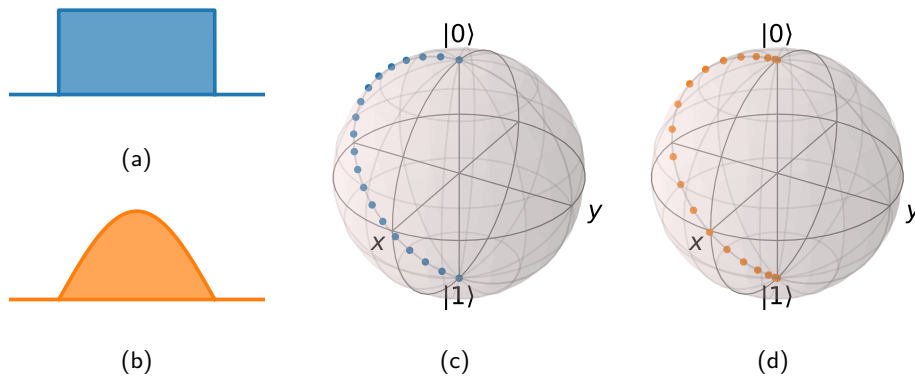


Figure 7: Discrete (a) and continuous (b) pulse coefficients. Both can be used to realize a π pulse that flips the qubit. The corresponding trajectory in the Bloch sphere is shown in (c) and (d). Points on the Bloch sphere are sampled with constant time steps. Although for both pulses the quantum states evolve along the same path, the speed is different and proportional to the pulse strength. On a real quantum hardware, a smooth control pulse usually reduces the leakage to the non-qubit subspace.

```

from qutip_qip.circuit import QubitCircuit
from qutip import sigmaz, sigmax, identity, tensor, basis

# Deutsch-Josza algorithm
dj_circuit = QubitCircuit(3)
dj_circuit.add_gate("X", targets=2)
dj_circuit.add_gate("SNOT", targets=0)
dj_circuit.add_gate("SNOT", targets=1)
dj_circuit.add_gate("SNOT", targets=2)

# Oracle function f(x)
dj_circuit.add_gate("CNOT", controls=0, targets=2)
dj_circuit.add_gate("CNOT", controls=1, targets=2)

dj_circuit.add_gate("SNOT", targets=0)
dj_circuit.add_gate("SNOT", targets=1)

# Spin chain model
spinchain_processor = LinearSpinChain(3, t2=30) # T2 = 30
spinchain_processor.load_circuit(dj_circuit)
initial_state = basis([2, 2, 2], [0, 0, 0]) # 3 qubits in the 000 state
t_record = np.linspace(0, 20, 300)
result1 = spinchain_processor.run_state(initial_state, tlist=t_record)

# Superconducting qubits
scqubits_processor = SCQubits(num_qubits)
scqubits_processor.load_circuit(dj_circuit)
initial_state = basis([3, 3, 3], [0, 0, 0]) # 3-level
result2 = scqubits_processor.run_state(initial_state)

# Optimal control model
setting_args = {"SNOT": {"num_tslots": 6, "evo_time": 2},
               "X": {"num_tslots": 1, "evo_time": 0.5},
               "CNOT": {"num_tslots": 12, "evo_time": 5}}
opt_processor = OptPulseProcessor(N=3)
opt_processor.add_control(sigmax(), cyclic_permutation=True)
opt_processor.add_control(sigmaz(), cyclic_permutation=True)
opt_processor.add_control(tensor([sigmax(), sigmax(), identity(2)]))
opt_processor.add_control(tensor([identity(2), sigmax(), sigmax()]))
opt_processor.load_circuit( # Provide parameters for the algorithm
    dj_circuit, setting_args=setting_args, merge_gates=False,

```

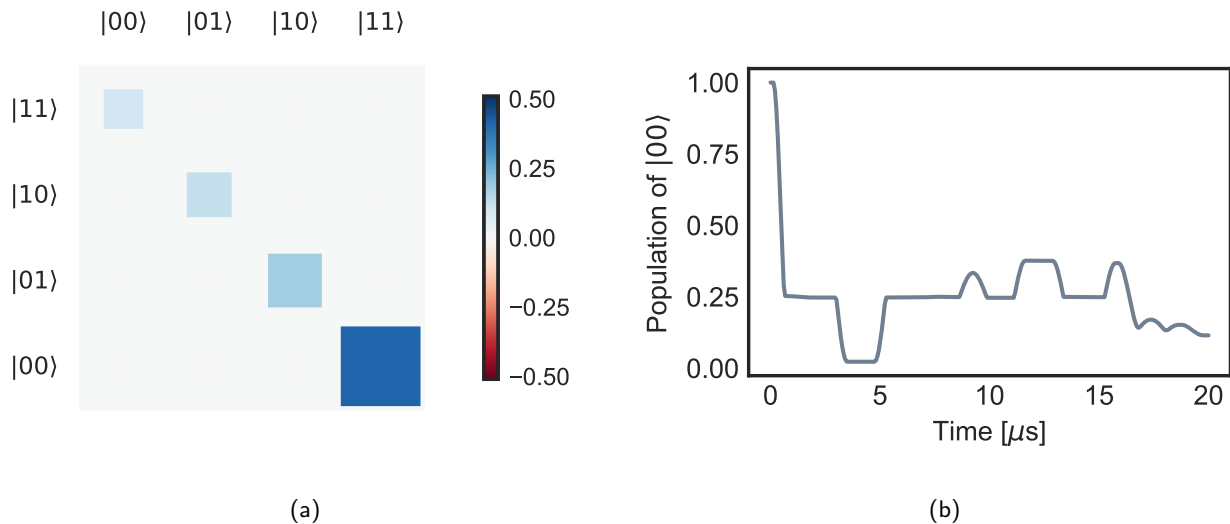


Figure 8: The Hinton diagram of the final density matrix (Figure 8a) and the population of the $|00\rangle$ state during the circuit execution (Figure 8b) for the first two qubits in the circuit shown in Figure 3. The Hinton diagram is a visual representation of the complex-valued density matrix. The shade and size of the blocks are determined by the absolute value of the density matrix element and the color blue (red) denotes whether the real part of the density matrix is positive (negative). For an ideal Deutsch-Jozsa algorithm with a balanced oracle. The first two qubits should end up having no overlap with the ground state. This is not exactly the case in the plot because we define a finite T_2 time.

```

verbose=True, amp_ubound=5, amp_lbound=0)
initial_state = basis([2, 2, 2], [0, 0, 0])
result3 = opt_processor.run_state(initial_state)

```

In the above code block, we first define the Deutsch-Jozsa algorithm, same as the circuit shown in Figure 3. We then run the circuit on various hardware models. For the spin model and superconducting qubits, a Hamiltonian model and a compiler are already predefined and one only needs to load the circuit and run the simulation. Hardware parameters, such as the T_1 and T_2 times, qubit frequencies and coupling strength, can be given as parameters to initialize the processor. For the optimal control model, we need to first define the available control Hamiltonians and also provide a few parameters for the optimization routine in QuTiP, such as the maximal pulse amplitude and the number of time slots for each gate. For details, please refer to the QuTiP documentation (<http://qutip.org/docs/latest/index.html>).

The generated control pulses are shown in Figure 3 and can be obtained by the method:

```
processor.plot_pulses()
```

Because we are doing a simulation, we have access both to the final states as a density matrix and the information of the states during the evolution. We demonstrate this in Figure 8. By construction, the measured result of the first two qubits of a perfect Deutsch-Jozsa algorithm with a balanced oracle should not overlap with the state $|00\rangle$. This agrees with the small population of the state $|00\rangle$ in the Hinton diagram (Figure 8a). The population is not exactly zero because we define a T_2 decoherence noise. In addition, we can also extract information during the circuit execution, e.g., the population as a function of time (Figure 8b).

C Customizing the physical model and noise

In the following, we show a minimal example of constructing Hamiltonian models and compilers:

```

import numpy as np
from qutip import sigmax, sigmay, sigmaz, basis, qeye, tensor, Qobj, fock_dm
from qutip_qip.circuit import QubitCircuit, Gate

```

```

from qutip_qip.device import ModelProcessor
from qutip_qip.compiler import GateCompiler, Instruction
from qutip import Options
from qutip_qip.noise import Noise

class MyProcessor(ModelProcessor):
    """Custom processor built using ModelProcessor as the base class.

    This custom processor will inherit all the methods of the base class
    such as setting up of the T1 and T2 decoherence rates in the simulations.

    In addition, it is possible to write your own functions to add control
    pulses.

    Args:
        num_qubits (int): Number of qubits in the processor.
        t1, t2 (float or list): The T1 and T2 decoherence rates for the
                               qubit. If it is a list, then it is assumed that
                               each element of the list corresponds to the rates
                               for each of the qubits.
    """

    def __init__(self, num_qubits, t1=None, t2=None):
        super().__init__(num_qubits, t1=t1, t2=t2)
        self.pulse_mode = "discrete" # set the control pulse as discrete or
                                     continuous.

        self.set_up_ops(num_qubits) # set up the available Hamiltonians.
        self.dims = [2] * num_qubits # dimension of the quantum system.
        self.num_qubits = num_qubits
        self.native_gates = ["RX", "RY"]

    def set_up_ops(self):
        """Sets up the single qubit control operators for each qubit."""
        for m in range(self.num_qubits):
            self.add_control(2 * np.pi * sigmax() / 2, m, label="sx" + str(m))
        for m in range(self.num_qubits):
            self.add_control(2 * np.pi * sigmay() / 2, m, label="sy" + str(m))

class MyCompiler(GateCompiler):
    """Custom compiler for generating pulses from gates using the base class
    GateCompiler.

    Args:
        num_qubits (int): The number of qubits in the processor
        params (dict): A dictionary of parameters for gate pulses such as
                       the pulse amplitude.
    """

    def __init__(self, num_qubits, params):
        super().__init__(num_qubits, params=params)
        self.params = params
        self.gate_compiler = {
            "ROT": self.rotation_with_phase_compiler,
            "RX": self.single_qubit_gate_compiler,
            "RY": self.single_qubit_gate_compiler,
        }

    def generate_pulse(self, gate, tlist, coeff, phase=0.0):
        """Generates the pulses.

        Args:

```

```

        gate (qutip_qip.circuit.Gate): A qutip Gate object.
        tlist (array): A list of times for the evolution.
        coeff (array): An array of coefficients for the gate pulses
        phase (float): The value of the phase for the gate.

Returns:
    Instruction (qutip_qip.compiler.instruction.Instruction): An instruction
    to implement a gate containing the control pulses.
    """
    pulse_info = [
        ("sx" + str(gate.targets[0]), np.cos(phase) * coeff),
        ("sy" + str(gate.targets[0]), np.sin(phase) * coeff),
    ]
    return [Instruction(gate, tlist, pulse_info)]

def single_qubit_gate_compiler(self, gate):
    """Compiles single qubit gates to pulses.

    Args:
        gate (qutip_qip.circuit.Gate): A qutip Gate object.

    Returns:
        Instruction (qutip_qip.compiler.instruction.Instruction): An instruction
        to implement a gate containing the control pulses.
        """
    # gate.arg_value is the rotation angle
    tlist = np.abs(gate.arg_value) / self.params["pulse_amplitude"]
    coeff = self.params["pulse_amplitude"] * np.sign(gate.arg_value)
    if gate.name == "RX":
        return self.generate_pulse(gate, tlist, coeff, phase=0.0)
    elif gate.name == "RY":
        return self.generate_pulse(gate, tlist, coeff, phase=np.pi / 2)

def rotation_with_phase_compiler(self, gate):
    """Compiles gates with a phase term.

    Args:
        gate (qutip_qip.circuit.Gate): A qutip Gate object.

    Returns:
        Instruction (qutip_qip.compiler.instruction.Instruction): An instruction
        to implement a gate containing the control pulses.
        """
    # gate.arg_value is the pulse phase
    tlist = self.params["duration"]
    coeff = self.params["pulse_amplitude"]
    return self.generate_pulse(gate, tlist, coeff, phase=gate.arg_value)

# Define a circuit and run the simulation
num_qubits = 1

circuit = QubitCircuit(1)
circuit.add_gate("RX", targets=0, arg_value=np.pi / 2)
circuit.add_gate("Z", targets=0)

myprocessor = MyProcessor(1)

mycompiler = MyCompiler(num_qubits, {"pulse_amplitude": 0.02})

myprocessor.load_circuit(circuit, compiler=mycompiler)
result = myprocessor.run_state(basis(2, 0))

```

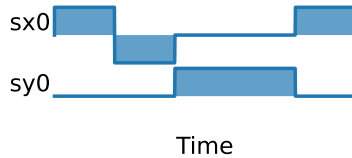


Figure 9: The compiled pulse of a $\pi/2$ pulse followed by a Z gate for the customized processor defined in appendix C. The Z gate is decomposed into rotations over the x and y axes.

In this example, we first build a Hamiltonian model called `MyProcessor`. For simplicity, we only include two single-qubit control Hamiltonians: σ_x and σ_y . Hence, rotations around the x and y axes are the native gates of our hardware. We then define the compiling routines for the two types of rotation gates. Providing this native gates set, rotation around z axis will be automatically decomposed into rotations around x and y axes. We define a circuit consisting of $\pi/2$ rotation followed by a Z gate. The compiled pulses are shown in Figure 9, where the Z gate is decomposed into rotations around x and y axes.

Next, we show an example of defining customized noise and simulating classical cross-talk:

```
class ClassicalCrossTalk(Noise):
    def __init__(self, ratio):
        self.ratio = ratio

    def get_noisy_dynamics(self, dims=None, pulses=None, systematic_noise=None):
        """Adds noise to the control pulses.

        Args:
            dims: Dimension of the system, e.g., [2,2,2,...] for qubits.
            pulses: A list of Pulse objects, representing the compiled pulses.
            systematic_noise: A Pulse object with no ideal control, used to represent
                pulse-independent noise such as decoherence (not used in this example).

        Returns:
            pulses: The list of modified pulses according to the noise model.
            systematic_noise: A Pulse object (not used in this example).
        """
        for i, pulse in enumerate(pulses):
            if "sx" or "sy" not in pulse.label:
                pass # filter out other pulses, e.g. drift
            target = pulse.targets[0]
            if target != 0: # add pulse to the left neighbour
                pulses[i].add_control_noise(
                    self.ratio * pulse.qobj,
                    targets=[target - 1],
                    coeff=pulse.coeff,
                    tlist=pulse.tlist,
                )
            if target != len(dims) - 1: # add pulse to the right neighbour
                pulses[i].add_control_noise(
                    self.ratio * pulse.qobj,
                    targets=[target + 1],
                    coeff=pulse.coeff,
                    tlist=pulse.tlist,
                )
        return pulses, systematic_noise

def single_crosstalk_simulation(num_gates):
    """ A single simulation, with num_gates representing the number of rotations.

    Args:
```

```

    num_gates (int): The random number of gates to add in the simulation.

Returns:
    result (qutip.solver.Result): A qutip Result object obtained from any of the
    solver methods such as mesolve.
"""
num_qubits = 2 # Qubit-0 is the target qubit. Qubit-1 suffers from crosstalk.
myprocessor = MyProcessor(num_qubits)
# Add qubit frequency detuning 1.852MHz for the second qubit.
myprocessor.add_drift(2 * np.pi * (sigmaz() + 1) / 2 * 1.852, targets=1)
myprocessor.native_gates = None # Remove the native gates
mycompiler = MyCompiler(num_qubits, {"pulse_amplitude": 0.02, "duration": 25})
myprocessor.add_noise(ClassicalCrossTalk(1.0))
# Define a random circuit.
gates_set = [
    Gate("ROT", 0, arg_value=0),
    Gate("ROT", 0, arg_value=np.pi / 2),
    Gate("ROT", 0, arg_value=np.pi),
    Gate("ROT", 0, arg_value=np.pi / 2 * 3),
]
circuit = QubitCircuit(num_qubits)
for ind in np.random.randint(0, 4, num_gates):
    circuit.add_gate(gates_set[ind])
# Simulate the circuit.
myprocessor.load_circuit(circuit, compiler=mycompiler)
init_state = tensor(
    [Qobj([[init_fid, 0], [0, 0.025]]), Qobj([[init_fid, 0], [0, 0.025]])]
)
options = Options(nsteps=10000) # increase the maximal allowed steps
e_ops = [tensor([qeye(2), fock_dm(2)])] # observable

# compute results of the run using a solver of choice with custom options
result = myprocessor.run_state(init_state, solver="mesolve",
    options=options, e_ops=e_ops)
result = result.expect[0][-1] # measured expectation value at the end
return result

```

In the code block above, we first define a custom `ClassicalCrossTalk` noise object that uses the `Noise` class as the base. The `get_noisy_dynamics` method will be called during the simulation to generate the noisy Hamiltonian model. Here, we define a noise model that adds the same driving Hamiltonian to its neighbouring qubits, with a strength proportional to the control pulses strength applied on it. The detuning of the qubit transition frequency is simulated by adding a σ_z drift Hamiltonian to the processor, with a frequency of 1.852 MHz.

Second, we define a random circuit consisting of a sequence of π rotation pulses with random phases. The driving pulse is a π pulse with a duration of 25 μs and Rabi frequency 20 KHz. As described in [49], this randomized benchmarking protocol allows one to study the classical cross-talk induced decoherence on the neighbouring qubits. The two qubits are initialized in the $|00\rangle$ state with a fidelity of 0.975. After the circuit, we measure the population of the second qubit. If there is no cross-talk, it will remain perfectly in the ground state. However, cross-talk induces a diffusive behaviour of the second qubit and the fidelity decreases. This simulation is repeated 1600 times to obtain the average fidelity, as shown in Figure 4 in the main text.

D Simulating QASM circuits

To allow using circuit optimization and scheduling techniques provided by other packages, we support the importation and exportation of quantum circuits in QASM format. As an example, we use again the 3-qubit Deutsch-Jozsa circuit (Figure 3). The code example to manually construct the circuit is shown in appendix B. Here, we show that the same quantum circuit can also be imported into QuTiP

using the QASM module. First, we describe the OpenQASM 2.0 program corresponding to the 3-qubit Deutsch-Jozsa circuit. The following block shows an example of a QASM file:

```
OPENQASM 2.0;
include "qelib1.inc";

qreg q[3];
x q[2];
h q;
cx q[0], q[2];
cx q[1], q[2];
h q[0];
h q[1];
```

The QASM file can be saved as a `.qasm` file (such as `"deutsch-jozsa.qasm"` in our example below). Every QASM file imported to QuTiP requires the two header statements at the beginning of the file. `OPENQASM 2.0` declares that the file adheres to the OpenQASM 2.0 standard. The keyword `include` processes a file that contains definitions of some QASM gates. It is available in the OpenQASM repository (as a standard file) and is included with the QASM file exported by QuTiP (and also by Qiskit/Cirq). This circuit can be easily imported into QuTiP using the `read_qasm` method in the following manner:

```
from qutip_qip.qasm import read_qasm

qc = read_qasm("deutsch-jozsa.qasm")
```

Furthermore, using the `strmode` option for `read_qasm` function, we can import the circuit described in a string object. Once a quantum circuit is defined, we can also export it to the QASM format and save it as a file using the `QubitCircuit.save_qasm` method:

```
from qutip_qip.qasm import save_qasm

save_qasm(qc, "deutsch-jozsa-qutip.qasm")
```

The circuit can then be simulated with other packages as required. There is also an option to output the circuit as a string using the `QubitCircuit.circuit_to_qasm_str` method or print it out using the `QubitCircuit.print_qasm` method.

References

- [1] J. Preskill, Quantum computing in the NISQ era and beyond, *Quantum* **2**, 79 (2018).
- [2] M. A. Nielsen and I. L. Chuang, *Quantum Computation and Quantum Information* (Cambridge University Press, 2000).
- [3] I. Buluta, S. Ashhab, and F. Nori, Natural and artificial atoms for quantum computation, *Rep. Prog. Phys.* **74**, 104401 (2011).
- [4] K. Bharti, A. Cervera-Lierta, T. H. Kyaw, T. Haug, S. Alperin-Lea, A. Anand, M. Degroote, H. Heimonen, J. S. Kottmann, T. Menke, W.-K. Mok, S. Sim, L.-C. Kwek, and A. Aspuru-Guzik, Noisy intermediate-scale quantum (NISQ) algorithms, *arXiv preprint* (2021), [arXiv:2101.08448](https://arxiv.org/abs/2101.08448).
- [5] R. S. Smith, M. J. Curtis, and W. J. Zeng, A Practical Quantum Instruction Set Architecture, *arXiv preprint* (2016), [arXiv:1608.03355](https://arxiv.org/abs/1608.03355).
- [6] P. J. Karalekas, N. A. Tezak, E. C. Peterson, C. A. Ryan, M. P. da Silva, and R. S. Smith, A quantum-classical cloud platform optimized for variational hybrid algorithms, *Quantum Sci. Technol.* **5**, 024003 (2020).
- [7] G. Aleksandrowicz, T. Alexander, P. Barkoutsos, L. Bello, Y. Ben-Haim, D. Bucher, F. J. Cabrera-Hernández, J. Carballo-Franquis, A. Chen, C.-F. Chen, J. M. Chow, *et al.*, *Qiskit: An Open-source Framework for Quantum Computing* (2019).
- [8] Cirq Developers, *Cirq* (2021), See full list of authors on Github: <https://github.com/quantumlib/Cirq/graphs/contributors>.
- [9] D. S. Steiger, T. Häner, and M. Troyer, ProjectQ: an open source software framework for quantum computing, *Quantum* **2**, 49 (2018).

- [10] V. Bergholm, J. Izaac, M. Schuld, C. Gogolin, M. S. Alam, S. Ahmed, J. M. Arrazola, C. Blank, A. Delgado, S. Jahangiri, *et al.*, PennyLane: Automatic differentiation of hybrid quantum-classical computations, [arXiv preprint \(2018\)](#), [arXiv:1811.04968](#).
- [11] M. Fingerhuth, T. Babej, and P. Wittek, Open source software in quantum computing, [PLOS ONE **13**, e0208561 \(2018\)](#).
- [12] B. Heim, M. Soeken, S. Marshall, C. Granade, M. Roetteler, A. Geller, M. Troyer, and K. Svore, Quantum programming languages, [Nat. Rev. Phys. **2**, 709 \(2020\)](#).
- [13] T. Alexander, N. Kanazawa, D. J. Egger, L. Capelluto, C. J. Wood, A. Javadi-Abhari, and D. C McKay, Qiskit pulse: Programming quantum computers through the cloud with pulses, [Quantum Sci. Technol. **5**, 044006 \(2020\)](#).
- [14] H. Ball, M. J. Biercuk, A. Carvalho, J. Chen, M. Hush, L. A. De Castro, L. Li, P. J. Liebermann, H. J. Slatyer, C. Edmunds, V. Frey, C. Hempel, and A. Milne, Software tools for quantum control: Improving quantum computer performance through noise and error suppression, [arXiv preprint \(2020\)](#), [arXiv:2001.04060](#).
- [15] H. Silvério, S. Grijalva, C. Dalyac, L. Leclerc, P. J. Karalekas, N. Shammah, M. Beji, L.-P. Henry, and L. Henriët, Pulser: An open-source package for the design of pulse sequences in programmable neutral-atom arrays, [arXiv preprint \(2021\)](#), [arXiv:2104.15044](#).
- [16] J. Johansson, P. Nation, and F. Nori, QuTiP: An open-source python framework for the dynamics of open quantum systems, [Comput. Phys. Commun. **183**, 1760 \(2012\)](#).
- [17] J. R. Johansson, P. D. Nation, and F. Nori, QuTiP 2: A Python framework for the dynamics of open quantum systems, [Comput. Phys. Commun. **184**, 1234 \(2013\)](#).
- [18] N. Shammah, S. Ahmed, N. Lambert, S. De Liberato, and F. Nori, Open quantum systems with local and collective incoherent processes: Efficient numerical simulations using permutational invariance, [Phys. Rev. A **98**, 063815 \(2018\)](#).
- [19] M. H. Goerz, D. Basilewitsch, F. Gago Encinas, M. G. Krauss, K. P. Horn, D. M. Reich, and C. P. Koch, Krotov: A Python implementation of Krotov’s method for quantum optimal control, [SciPost Phys. **7**, 80 \(2019\)](#).
- [20] N. Lambert, S. Ahmed, M. Cirio, and F. Nori, Modelling the ultra-strongly coupled spin-boson model with unphysical modes, [Nat. Commun. **10**, 3721 \(2019\)](#).
- [21] N. Lambert, T. Raheja, S. Ahmed, A. Pitchford, and F. Nori, BoFiN-HEOM: A bosonic and fermionic numerical hierarchical-equations-of-motion library with applications in light-harvesting, quantum control, and single-molecule electronics, [arXiv preprint \(2020\)](#), [arXiv:2010.10806](#).
- [22] [qopt: A simulation and quantum optimal control package, <https://github.com/qutech/qopt>](#).
- [23] N. Khaneja, T. Reiss, C. Kehlet, T. Schulte-Herbrüggen, and S. J. Glaser, Optimal control of coupled spin dynamics: Design of NMR pulse sequences by gradient ascent algorithms, [J. Magn. Reson. **172**, 296 \(2005\)](#).
- [24] L. B.-V. Horn, [sequencing-dev/sequencing: v1.1.3 \(2021\)](#).
- [25] C. R. Harris, K. J. Millman, S. J. van der Walt, R. Gommers, P. Virtanen, D. Cournapeau, E. Wieser, J. Taylor, S. Berg, N. J. Smith, *et al.*, Array programming with NumPy, [Nature **585**, 357 \(2020\)](#).
- [26] P. Virtanen, R. Gommers, T. E. Oliphant, M. Haberland, T. Reddy, D. Cournapeau, E. Burovski, P. Peterson, W. Weckesser, J. Bright, *et al.*, SciPy 1.0: fundamental algorithms for scientific computing in Python, [Nat. Methods **17**, 261 \(2020\)](#).
- [27] J. D. Hunter, Matplotlib: A 2D graphics environment, [Comput. Sci. Eng. **9**, 90 \(2007\)](#).
- [28] S. Behnel, R. Bradshaw, C. Citro, L. Dalcin, D. S. Seljebotn, and K. Smith, Cython: The best of both worlds, [Computing in Science & Engineering **13**, 31 \(2011\)](#).
- [29] The full list of qutip-qip contributors, <https://github.com/qutip/qutip-qip/graphs/contributors> (2021).
- [30] H.-P. Breuer and F. Petruccione, *The theory of open quantum systems* (Oxford University Press, 2002).
- [31] D. A. Lidar, Lecture Notes on the Theory

- of Open Quantum Systems, [arXiv preprint \(2019\)](#), [arXiv:1902.00967](#).
- [32] Y. Tanimura and R. Kubo, Time evolution of a quantum system in contact with a nearly Gaussian-Markoffian noise bath, *J. Phys. Soc. Jpn.* **58**, 101 (1989).
- [33] P. Mundada, G. Zhang, T. Hazard, and A. Houck, Suppression of qubit crosstalk in a tunable coupling superconducting circuit, *Phys. Rev. Appl.* **12**, 054023 (2019).
- [34] E. Magesan and J. M. Gambetta, Effective Hamiltonian models of the cross-resonance gate, *Phys. Rev. A* **101**, 052308 (2020).
- [35] D. D'Alessandro, *Introduction to Quantum Control and Dynamics* (Chapman & Hall/CRC, 2007).
- [36] D. Loss and D. P. DiVincenzo, Quantum computation with quantum dots, *Phys. Rev. A* **57**, 120 (1998).
- [37] B. E. Kane, A silicon-based nuclear spin quantum computer, *Nature* **393**, 133 (1998).
- [38] P. Krantz, M. Kjaergaard, F. Yan, T. P. Orlando, S. Gustavsson, and W. D. Oliver, A quantum engineer's guide to superconducting qubits, *Appl. Phys. Rev.* **6**, 021318 (2019).
- [39] X. Gu, A. F. Kockum, A. Miranowicz, Y.-X. Liu, and F. Nori, Microwave photonics with superconducting quantum circuits, *Phys. Rep.* **718-719**, 1 (2017).
- [40] A. F. Kockum and F. Nori, Quantum bits with Josephson junctions, in *Fundamentals and Frontiers of the Josephson Effect*, edited by F. Tafuri (Springer, 2019) p. 703.
- [41] C. Rigetti and M. Devoret, Fully microwave-tunable universal gates in superconducting qubits with linear couplings and fixed transition frequencies, *Phys. Rev. B* **81**, 134507 (2010).
- [42] S. Machnes, U. Sander, S. J. Glaser, P. de Fouquières, A. Gruslys, S. Schirmer, and T. Schulte-Herbrüggen, Comparing, optimizing, and benchmarking quantum-control algorithms in a unifying programming framework, *Phys. Rev. A* **84**, 022305 (2011).
- [43] T. Caneva, T. Calarco, and S. Montangero, Chopped random-basis quantum optimization, *Phys. Rev. A* **84**, 022326 (2011).
- [44] P. Doria, T. Calarco, and S. Montangero, Optimal control technique for many-body quantum dynamics, *Phys. Rev. Lett.* **106**, 190501 (2011).
- [45] D. Maslov, G. Dueck, D. Miller, and C. Negrevergne, Quantum circuit simplification and level compaction, *IEEE Trans. Comput. Des. Integr. Circuits Syst.* **27**, 436 (2008).
- [46] A. Javadiabhari, S. Patil, D. Kudrow, J. Heckey, A. Lvov, F. T. Chong, and M. Martonosi, ScaffCC: Scalable compilation and analysis of quantum programs, *Parallel Comput.* **45**, 2 (2015).
- [47] T. Häner, D. S. Steiger, K. Svore, and M. Troyer, A software methodology for compiling quantum programs, *Quantum Sci. Technol.* **3**, 020501 (2018).
- [48] T. Fösel, M. Y. Niu, F. Marquardt, and L. Li, Quantum circuit optimization with deep reinforcement learning, [arXiv preprint \(2021\)](#), [arXiv:2103.07585](#).
- [49] C. Piltz, T. Sriarunothai, A. Varón, and C. Wunderlich, A trapped-ion-based quantum byte with 10^{-5} next-neighbour crosstalk, *Nat. Commun.* **5**, 4679 (2014).
- [50] A. W. Cross, L. S. Bishop, J. A. Smolin, and J. M. Gambetta, Open Quantum Assembly Language, [arXiv preprint \(2017\)](#), [arXiv:1707.03429](#).
- [51] N. Khammassi, G. G. Guerreschi, I. Ashraf, J. W. Hogaboam, C. G. Almudever, and K. Bertels, cqasm v1. 0: Towards a common quantum assembly language, [arXiv preprint \(2018\)](#), [arXiv:1805.09607](#).
- [52] L. S. Bishop, Qasm 2.0: A quantum circuit intermediate representation, in *APS March Meeting Abstracts*, Vol. 2017 (2017) p. 46.
- [53] M. Alam, A. Ash-Saki, and S. Ghosh, Accelerating quantum approximate optimization algorithm using machine learning, in *2020 Des. Autom. Test Eur. Conf. Exhib. (DATE)* (2020) p. 686.
- [54] T. Haug and M. S. Kim, Optimal training of variational quantum algorithms without barren plateaus, [arXiv preprint \(2021\)](#), [arXiv:2104.14543](#).
- [55] P. Murali, J. M. Baker, A. Javadi-Abhari, F. T. Chong, and M. Martonosi, Noise-adaptive compiler mappings for noisy intermediate-scale quantum computers, in *Proc. 24th Int. Conf. Archit. Support Program. Lang. Oper. Syst.* (ACM, 2019) p. 1015.

- [56] A. Kandala, K. Temme, A. D. Córcoles, A. Mezzacapo, J. M. Chow, and J. M. Gambetta, Error mitigation extends the computational reach of a noisy quantum processor, *Nature* **567**, 491 (2019).
- [57] T. Giurgica-Tiron, Y. Hindy, R. LaRose, A. Mari, and W. J. Zeng, Digital zero noise extrapolation for quantum error mitigation, *Proc. - IEEE Int. Conf. Quantum Comput. Eng. QCE 2020* (2020).
- [58] R. LaRose, A. Mari, P. J. Karalekas, N. Shammah, and W. J. Zeng, Mitiq: A software package for error mitigation on noisy quantum computers, *arXiv preprint* (2020), [arXiv:2009.04417](https://arxiv.org/abs/2009.04417).
- [59] K. Schultz, G. Quiroz, P. Titum, and B. Clader, SchWARMA: A model-based approach for time-correlated noise in quantum circuits, *arXiv preprint* (2020), [arXiv:2010.04580](https://arxiv.org/abs/2010.04580).
- [60] S. Humpohl, L. Prediger, P. Bethke, A. Willmes, J. Bergmann, M. Meyer, E. Kammerloher, L. Lankes, T. Hangleiter, P. Eendebak, and P. Cerfontaine, *qutech/qupulse: qupulse 0.5.1* (2020).
- [61] N. Wittler, F. Roy, K. Pack, M. Werninghaus, A. S. Roy, D. J. Egger, S. Filipp, F. K. Wilhelm, and S. Machnes, Integrated Tool Set for Control, Calibration, and Characterization of Quantum Devices Applied to Superconducting Qubits, *Phys. Rev. Appl.* **15** (2021).
- [62] B. Skinner, J. Ruhman, and A. Nahum, Measurement-induced phase transitions in the dynamics of entanglement, *Phys. Rev. X* **9**, 031009 (2019).
- [63] M. S. Blok, V. V. Ramasesh, T. Schuster, K. O’Brien, J. M. Kreikebaum, D. Dahlen, A. Morvan, B. Yoshida, N. Y. Yao, and I. Siddiqi, Quantum information scrambling on a superconducting qutrit processor, *Phys. Rev. X* **11**, 021010 (2021).
- [64] S. Machnes, E. Assémat, D. Tannor, and F. K. Wilhelm, Tunable, Flexible, and Efficient Optimization of Control Pulses for Practical Qubits, *Phys. Rev. Lett.* **120**, 150401 (2018).
- [65] D. Dong, C. Chen, B. Qi, I. R. Petersen, and F. Nori, Robust manipulation of superconducting qubits in the presence of fluctuations, *Sci. Rep.* **5**, 7873 (2015).
- [66] D. Dong, C. Wu, C. Chen, B. Qi, I. R. Petersen, and F. Nori, Learning robust pulses for generating universal quantum gates, *Sci. Rep.* **6**, 36090 (2016).
- [67] A. W. Cross, A. Javadi-Abhari, T. Alexander, N. de Beaudrap, L. S. Bishop, S. Heidel, C. A. Ryan, J. Smolin, J. M. Gambetta, and B. R. Johnson, OpenQASM 3: A broader and deeper quantum assembly language, *arXiv preprint* (2021), [arXiv:2104.14722](https://arxiv.org/abs/2104.14722).